Molecular Genetics and Genomics (2024) 299:13
https://doi.org/10.1007/s00438-024-02102-z

ORIGINAL ARTICLE

Mechanism underlying the rapid growth of *Phalaenopsis equestris* induced by ^{60}Co-γ-ray irradiation

Yang Meng[1,2] · Wei Li[1,2] · Yunxiao Guan[3] · Zihan Song[1,2] · Guoren He[1,2] · Donghui Peng[3] · Feng Ming[1,2]

Received: 1 July 2023 / Accepted: 11 January 2024

Abstract

Gamma (γ)-ray irradiation is one of the important modern breeding methods. Gamma-ray irradiation can affect the growth rate and other characteristics of plants. Plant growth rate is crucial for plants. In horticultural crops, the growth rate of plants is closely related to the growth of leaves and flowering time, both of which have important ornamental value. In this study, ^{60}Co-γ-ray was used to treat *P. equestris* plants. After irradiation, the plant's leaf growth rate increased, and sugar content and antioxidant enzyme activity increased. Therefore, we used RNA-seq technology to analyze the differential gene expression and pathways of control leaves and irradiated leaves. Through transcriptome analysis, we investigated the reasons for the rapid growth of *P. equestris* leaves after irradiation. In the analysis, genes related to cell wall relaxation and glucose metabolism showed differential expression. In addition, the expression level of genes encoding ROS scavenging enzyme synthesis regulatory genes increased after irradiation. We identified two genes related to P. equestris leaf growth using VIGS technology: *PeNGA* and *PeEXPA10*. The expression of *PeEXPA10,* a gene related to cell wall expansion, was down-regulated, cell wall expansion ability decreased, cell size decreased, and leaf growth rate slowed down. The TCP-NGATHA (NGA) molecular regulatory module plays a crucial role in cell proliferation. When the expression of the *PeNGA* gene decreases, the leaf growth rate increases, and the number of cells increases. After irradiation, *PeNGA* and *PeEXPA10* affect the growth of *P. equestris* leaves by influencing cell proliferation and cell expansion, respectively. In addition, many genes in the plant hormone signaling pathway show differential expression after irradiation, indicating the crucial role of plant hormones in plant leaf growth. This provides a theoretical basis for future research on leaf development and biological breeding.

Keywords *Phalaenopsis equestris* · ^{60}co-γ-ray irradiation · Rapid growth · Transcriptome analysis · Leaf development

Introduction

Orchids are horticultural plants with important ornamental value and economic value (Li et al. 2021). Belonging to one of the largest families of angiosperms, orchids encompass approximately 880 genera and 27,800 species (Givnish et al. 2016). Phalaenopsis equestris, known as the "Queen of Orchids," is globally cultivated (Lin et al. 2016; Zhang et al. 2018). Irradiation mutagenesis breeding, characterized by high variation frequencies and diverse variations, enables the production of stable offspring within a short breeding period. This method can induce changes in plant morphology, physiology, and biochemistry, leading to the development of new varieties with unique traits that are not achievable through other breeding methods. Consequently, it has been widely utilized for enhancing horticultural crops (Yamaguchi 2018). Among the mutagens used for this type of breeding, γ-ray is considered to be the most effective (Kovacs and Keresztes

Yang Meng is the sole first author.

Communicated by Bing Yang.

✉ Donghui Peng
fjpdh@fafu.edu.cn

✉ Feng Ming
fming@fudan.edu.cn

1 Development Centre of Plant Germplasm Resources, College of Life Sciences, Shanghai Normal University, 100 Guilin Road, Xuhui District, Shanghai 200234, China

2 Shanghai Key Laboratory of Plant Molecular Sciences, College of Life Sciences, Shanghai Normal University, Shanghai 200234, China

3 Present Address: Key Laboratory of National Forestry and Grassland Administration for Orchid Conservation and Utilization at College of Landscape Architecture and Art, Fujian Agriculture and Forestry University, Fuzhou 350002, China

Published online: 23 February 2024

2002). It can affect the process of plant growth and development. However, the molecular mechanisms underlying the changes in plant phenotypes induced by gamma irradiation have been little explored.

Low-dose irradiation has been shown to stimulate various physiological metabolic processes in cells, including increased enzyme activities, photosynthetic and respiratory rates, growth promotion, and enhanced immunity (Calabrese and Baldwin 2000; Upton 2001). In tomatoes, low-dose irradiation has been found to promote flowering and early fruit set (Alarkon et al. 1987) and stimulate stem growth, root branching, and root length in tissue culture seedlings (Charbaji and Nabulsi 1999). Similarly, low-dose irradiation has been reported to increase the growth rate, height, and fresh weight of wheat (Singh and Datta 2010), as well as accelerate the growth of rice and mung beans, resulting in increases in plant height, number of inflorescences, tillering, and number and length of pods and seeds (Maity et al. 2005).

The leaf, as the primary photosynthetic organ of plants, exhibits significant variations in morphology across different species, developmental stages, and growth conditions (Tsukaya 2014). Leaves play a crucial role in contributing to plant biomass, as the energy and carbohydrates produced during photosynthesis support the plant's growth and life cycle (Demura and Ye 2010). After the establishment of leaf polarity in most plants, the leaf undergoes cell proliferation and expansion to attain its final size and shape (Yamaguchi et al. 2010). Leaf initiation begins with a group of primitive initiating cells that emerge laterally in the shoot apical meristem (Kalve et al. 2014). These primitive cells within the leaf primordia undergo extensive cell division, leading to an increase in the number of cells that ultimately determine the size of the leaf (Gonzalez et al. 2012). The cell wall, primarily composed of cellulose and pectin, serves as the interface between protoplasts and the extracellular environment in plant cells. It plays a crucial role in perceiving external changes and influences morphological characteristics and mechanical properties during growth and development (Szymanski and Cosgrove 2009; Somerville et al. 2004). Deletion of cellulase in Arabidopsis thaliana mutants leads to reduced cellulose contents, as well as decreased leaf and cotyledon areas (Williamson et al. 2001). Pectin is essential for cell growth and tissue morphological development (Anderson 2016, 2019). Transcription factors associated with various hormone pathways, such as abscisic acid, gibberellin, auxin, and cytokinin pathways, play significant roles in plant leaf development (Saidi and Hajibarat 2021). *PeEXPA10* is an expansion that contributes to cell wall expansion and affects leaf growth and development by modulating the cell wall structure. The ectopic expression of *EXP10* in *A. thaliana* increases the size of leaves and cells and the length of petioles, whereas the down-regulated expression of *EXP10* has the opposite effects (Cosgrove 2015). In addition, the TCP family of transcription factors can regulate plant leaf morphology by affecting cell proliferation and differentiation (Aguilar-Martínez and Sinha 2013). NGA genes have a more general role in controlling lateral organ growth. TCP-NGA regulatory interactions may be conserved in angiosperms, including important crop species, and the regulation of leaf development is an important mechanism (Ballester et al. 2015). The leaves of the Arabidopsis nga mutant are wider and shorter than those of the wild type, and these phenotypes are also observed in other floral organs, especially sepals and petals (Fourquin and Ferrándiz 2014).In contrast, NGA overexpression produced small, narrow leaves and petals (Alvarez et al. 2009; Kwon et al. 2009; Trigueros et al. 2009). Some mir319-regulated TCP factors are activators of NGA expression, and NGA factors mediate the role of TCP in leaf morphogenesis to some extent. In Arabidopsis, TCP2 and TCP3, which belong to the CIN branch of the TCP family, are targets of miR319. TCP2 and TCP3 are able to activate the NGA3 promoter. And this TCP-NGA regulatory module appears to be conserved in distantly related species, including crops such as tomato, rice or soybean (Ballester et al. 2015).

In this study, *P. equestris* plants were irradiated with ^{60}Co-γ-rays (40 Gy), which increased the soluble sugar content, antioxidant capacity, and leaf growth rate. The genes that were DEGs involved in leaf development and growth were screened. Additionally, the expression patterns and functions of *PeNGA* and *PeEXPA10* were examined. This study revealed the molecular mechanism underlying the rapid growth of irradiated *P. equestris* plants. The generated data may be useful for optimizing the γ-ray mutagenesis of *P. equestris* cultivars and the selection of new germplasm with ideal traits.

Materials and methods

Plant growth conditions and irradiation treatment

The irradiated materials were from the greenhouse of the Plant Germplasm Resources Center of Shanghai Normal University. Twelve *P. equestris* of the same growth period were selected, 6 of which were used as control (CK-1, CK-2, CK-3, CK-4, CK-5, CK-6), and 6 of which were used for radiation treatment (FZ- 40 Gy-1, FZ-40 Gy-2, FZ-40 Gy-3, Fz-40 Gy-4, FZ-40 Gy-5, FZ-40 Gy-6). Irradiation treatment: a dose of 40 Gy using ^{60}Co-γ-rays, with a dose rate of 150 Gy/h and an irradiation time of 16 min, was employed in the beam energy Irradiation Center of Shanghai Academy of Agricultural Sciences. Three strains of *P equestris* of CK and three strains of *P equestris* treated with 40 Gy were used for RNA-seq analysis.

P.equestris was cultivated under the standard greenhouse conditions, sunshine maintained for 12–14 h per day with the light intensity in 12,000–20000 lx; the temperature was set at 23 ˚C–27 ˚C; the relative humidity in the greenhouse was maintained at 60–80%.

P. equestris were used for VIGS gene silencing experiment, in the same growth period, and the number of infected plants was $n > 10$, respectively. Under the same growth conditions, the new leaves were observed, and the leaf growth data were recorded every seven days.

Determination of physiological indexes

Malondialdehyde (MDA) content determination (spectrophotometric method) (Li et al. 2000); Superoxide dismutase (SOD) activity (Lolium tetrazolium colourimetric method) (Li et al. 2000); Peroxidase (POD) activity (guaiacol method) (Li et al. 2000); Catalase (CAT) activity(ultraviolet absorption (UV)) (Li et al. 2000);Soluble sugar content (ananthous colourimetric method) (Wei et al. 2014).

RNA-seq

We collected leaves, which are characterized by rapid growth and wild-type, for RNA-seq analysis. RNA purification, reverse transcription, library construction, and sequencing were performed at Shanghai Majorbio Biopharm Biotechnology Co., Ltd.

According to the manufacturer's instructions, using an Illumina TruSeqTM RNA Sample Preparation Kit (San Diego, CA, USA), we prepared the RNA-Seq transcriptome libraries, which were then sequenced in a single lane on an Illumina Hiseq ten/NovaSeq 6000 sequencer for 2 × 150 bp paired-end reads. The RNA-seq raw read data were processed using the software fastx_toolkit_0.0.14 (http://hannonlab.cshl.edu/fastx_toolkit/), SeqPrep (https://github.com/jstjohn/SeqPrep), and Sickle (https://github.com/najoshi/sickle) to evaluate and discard sequences of low quality and those affected by adaptor contamination. Quality control is shown in Supplementary Data Table 1,4. The clean reads were mapped to the reference genome sequence of *P equestris*. NR, Swiss-Prot, Pfam, COG, GO, and KEGG databases were used for gene annotation.

RNA sequencing data were uploaded to the NCBI database (accession number PRJNA899319). Expression data were converted to FPKM values and gene expression differences were calculated using TBtools Biologist software, with heat maps displayed in red and blue showing high and weak expression of genes, respectively.

Quantification of gene expression levels

HISAT2 (http://ccb.jhu.edu/software/hisat2/index.shtml) was used to count the number of reads mapped to each gene. The Read Counts of each sample gene/transcript were obtained using the results of the comparison to the genome as well as the genome annotation file. They were then converted to FPKM, which led to the normalized gene/transcript expression levels.

Differential expression analysis

Based on the results of expression quantification, differential gene analysis between groups was performed to obtain genes that were differentially expressed between the two groups, with the differential analysis software: DESeq2, and the screening threshold: $|\log2FC| >= 1$ & padjust < 0.05(Qi et al. 2020; Anders and Huber 2012).

GO and KEGG enrichment analysis of DEGs

GO enrichment analysis of genes/transcripts in the gene set was performed using the software Goatools (https: //github.com/tanghaibao/GOatools), which is usually corrected for p-values by default and considered significantly enriched when the corrected *P*-value (FDR) is < 0.05 (Young et al. 2010). The KEGG PATHWAY enrichment analysis was performed by scripting the genes/transcripts in the gene set using the same principle as GO functional enrichment analysis.

Functional verification of virus-induced gene silencing (VIGS)

A specific fragment (300 bp) of *PeEXPA10*, *PeNGA* gene close to the 3´ end was inserted into the pCymMv vector by homologous recombination using ClonExpress®II One Step Cloning Kit (Vazyme Biotech). The VIGS silencing vectors pCymMv -PeEXPA10 and pCymMv -PeNGA were constructed. The recombinant expression transformants were placed in 5 ml of LB medium containing 100 µM Acetosyringone and 50 µg/ml kanamycin, so as to complete the activation of Agrobacterium cells, which were then cultured at 28℃ and 200 rpm for 13–16 h. When the OD600 of Agrobacterium cells reached 0.8–1.0, we suspended the cell pellet of Agrobacterium in 300 µl MS medium, and then we added 100 µM Acetosyringone to the MS medium and resuspended the cell pellet. Finally, we injected suspension into the leaves of Phalaenopsis. The plant materials were cultured for 30–40 days, accompanied by the continuous observation of leaves. Then the

infection was placed in an appropriate culture environment to observe the growth of new leaves.

Observation of growth rate

The leaf growth rate of the plants was observed using a consistent method. The data on leaf length and width of plants before irradiation were recorded in the irradiation experiment. Then, the data on the length and width of the leaves were recorded after ten days of growth. The area was estimated from literature reports ($S = 0.375L^2$; S, Square; L, Length) (Zhang et al. 2016), and then the ratio obtained using the area after ten days/area after irradiation was used as data for growth rate.

Similarly, in the VIGS experiment, the length and width of the leaves were recorded at 7-day intervals after VIGS infestation, and then the area was estimated using the same method. The data of leaf growth rate were obtained by dividing the area of 7D, 14D, 21D, 28D, 35D by the area of 0D, and were analyzed and made through the drawing software of PRISM.

Observation of epidermal cells

The newly born leaves of pCymMv silencing lines and CK were selected. Some epidermal tissues were cut on the leaf epidermis with a cutting knife, then placed on a slide with water, and covered with the cover glass to make simple plant tissue sections. The plant tissue section was placed on the microscope table to be observed with a 40 × lens, and the picture was saved. The cell number was counted, the more complete epidermal cells that could be seen in the microscopic field were counted as the whole number, while the epidermal cells with more defective shapes were not counted, and the data were repeated 10 times and three sets of reasonable data were selected as the final data, and the data were analyzed and made through the drawing software of PRISM.

RNA extraction and qPCR

The latest leaves of *Phalaenopsis* at different developmental stages (S0-S4) were collected to detect gene expression. RNA was extracted by mixing CK and irradiated plant samples. Total RNA was extracted using a SteadyPure Plant RNA Extraction Kit (Code: AG21019; Accurate Biotechnology Co., Ltd., Hunan, China). cDNA synthesis was performed with the RT reagent kit (Takara) according to the manufacturer's protocol. Real-time PCRs were done on a Chromo 4™ continuous fluorescence detector with the SYBR RT-PCR Kit (Takara) in a 20 µL reaction volume, which contained 10 µL of SYBR Green I PCR mix, 0.5 µM each of forward and reverse primer, 1 µL of cDNA template and appropriate amounts of sterile ddH_2O. Amplification conditions were: 2 min at 95 ◦C; 40 cycles of 15 s at 95 ◦C, 30 s at 58 ◦C, and 30 s at 72 ◦C. Fold changes of RNA transcripts were calculated by the $2 - \Delta\Delta Ct$ method. We used *PeActin* as the internal control. The entire experiment was repeated three times. Primers used in the qPCR were listed in Supplementary Data Table 5.

Results

Leaf growth was accelerated and physiological metabolism was enhanced after the irradiation with ^{60}Co-γ-rays

P. equestris plants were irradiated with ^{60}Co-γ-rays at a dose of 40 Gy and then maintained in a greenhouse to monitor their growth. At 10 days post-irradiation, the leaf growth rate of the irradiated group was significantly higher than that of the CK (Fig. 1A). Similarly, the SOD, POD, and CAT activities as well as the malondialdehyde and soluble sugar contents were significantly higher in the irradiated group than in the CK (Fig. 1B).

Identification of DEGs in irradiated leaves

To explore how irradiation promoted the growth and development of *P. equestris* leaves, a transcriptome sequencing analysis was performed using the *P. equestris* plants irradiated with a 40 Gy dose.

The transcriptome sequencing of 6 samples (CK, FZ, respectively, three repetitions) was completed and a total of 47.5 Gb Clean Data was obtained, with each sample reaching over 7.67 Gb Clean Data and the percentage of Q30 bases above 94.42%. The statistical power of this experimental design, calculated in RNASeqPower is 0.867.

Three replicates of the control and irradiated groups were analyzed and the transcriptome sequencing error was small (Supplementary Table S1). The principal component analysis of the RNA-seq data (Fig. 2A) detected obvious differences between the irradiated group and the CK. Moreover, the repeatability was relatively high. The correlation and cluster analyses of the six samples showed that the control material and the irradiated material formed separate clusters (Fig. 2B), indicating that the transcriptome data were appropriate for the subsequent analysis.

A total of 16,908 genes were identified in the irradiated group and the non-irradiated CK of which 15,521 genes were co-expressed, 570 genes were specifically expressed in CK, and 817 genes were specifically expressed in the irradiated group (Fig. 2C). The volcano plot indicated that the expression level changes were greater for the up-regulated genes in the control and irradiated groups than for the down-regulated

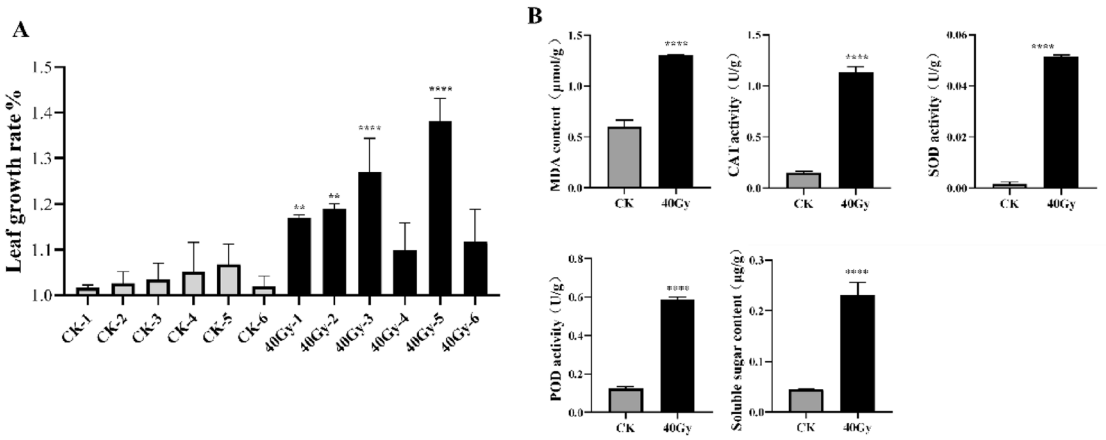

Fig. 1 Effect of ^{60}Co-γ-40 Gy irradiation on the growth of P. equestris leaves. **A** Comparison of growth rates between CK and 10 days after irradiation. **B** Analysis of physiological indexes of leaves after irradiation with ^{60}Co-γ-40 Gy. An asterisk (*) in-dicates significant differences among treatments (*$p<0.05$; **$p<0.01$. ***$p<0.001$. ****$p<0.0001$). All data were represented as means ± standard deviations (triplicate). Error bars indicate the standard error of the mean

genes (Fig. 2, D). There were 1070 DEGs, including 774 up-regulated genes and 296 down-regulated genes.

The proportions of alternative splicing events were as follows (Fig. 2E): skipped exon (SE), 37.7953%; retained intron (RI), 7.6990%; alternative 5′ splice site (A5SS), 15.6605%; alternative 3′ splice site (A3SS), 33.8583%; and mutually exclusive exon (MXE), 4.9869%. Thus, the most common alternative splicing events were SE and A3SS, which may have resulted in changes to protein structures and functions and altered plant growth.

Functional classification of DEGs according to GO and KEGG analyses

To characterize the genes induced by irradiation, the DEGs were functionally annotated on the basis of enriched GO terms and KEGG pathways. The GO enrichment analysis (Fig. 3A) classified the DEGs into the three main GO categories (molecular function, cellular component, and biological process). The 466 genes in the biological process category were annotated with various GO terms, including "detoxification," "developmental process," "response to stimulus," "cellular component organization or biogenesis," "biological regulation," "localization," "cellular process," and "metabolic process." The KEGG pathway analysis divided the DEGs in the irradiated and CK into the following five main categories (Fig. 3, B): "metabolism," "genetic information processing," "environmental information processing," "cellular processes," and "organismal systems." A total of 151 up-regulated genes and 111 down-regulated genes were classified. The main enriched pathways related to "metabolism" were "amino acid metabolism," "biosynthesis of other secondary metabolites," "carbohydrate metabolism," and "lipid metabolism." The main enriched pathways in the "genetic information processing" category were "folding, sorting and degradation," "replication and repair," and "translation." The enriched "environmental information processing" pathways were "membrane transport" and "signal transduction." Only one enriched pathway was detected in the "cellular processes" ("transport and catabolism") and "organismal systems" ("environmental adaptation") categories.

The DEGs between the CK and irradiated samples were classified by GO and KEGG enrichment analyses. The significantly enriched GO terms were "external encapsulating structure organization," "cell wall organization," "extracellular region," "cell wall," "external encapsulating structure," "plant-type cell wall," "carbohydrate metabolic process," "polysaccharide metabolic process," "cellular carbohydrate metabolic process," and "cell wall organization or biogenesis." More specifically, 52, 23, and 23 genes were annotated with "carbohydrate metabolic process," "cell wall," and "external encapsulating structure," respectively (Fig. 4A). The significantly enriched KEGG pathways were "nitrogen metabolism," "tropane, piperidine, and pyridine alkaloid biosynthesis," "plant hormone signal transduction," "pentose and glucuronate interconversions," "cysteine and methionine metabolism," "ether lipid metabolism," "cutin, suberin and wax biosynthesis," "steroid biosynthesis," "tyrosine metabolism," and "phenylpropanoid biosynthesis." A total of 18, 13, 10, and 10 genes were assigned to the "plant hormone signal transduction," "phenylpropanoid biosynthesis," "pentose and glucuronate interconversions," and "cysteine and methionine metabolism" pathways (Fig. 4B).

Combined analysis of RNA-seq data and physiological indices

To explore the reasons for the increased activities of the ROS-scavenging enzymes in the leaves following the

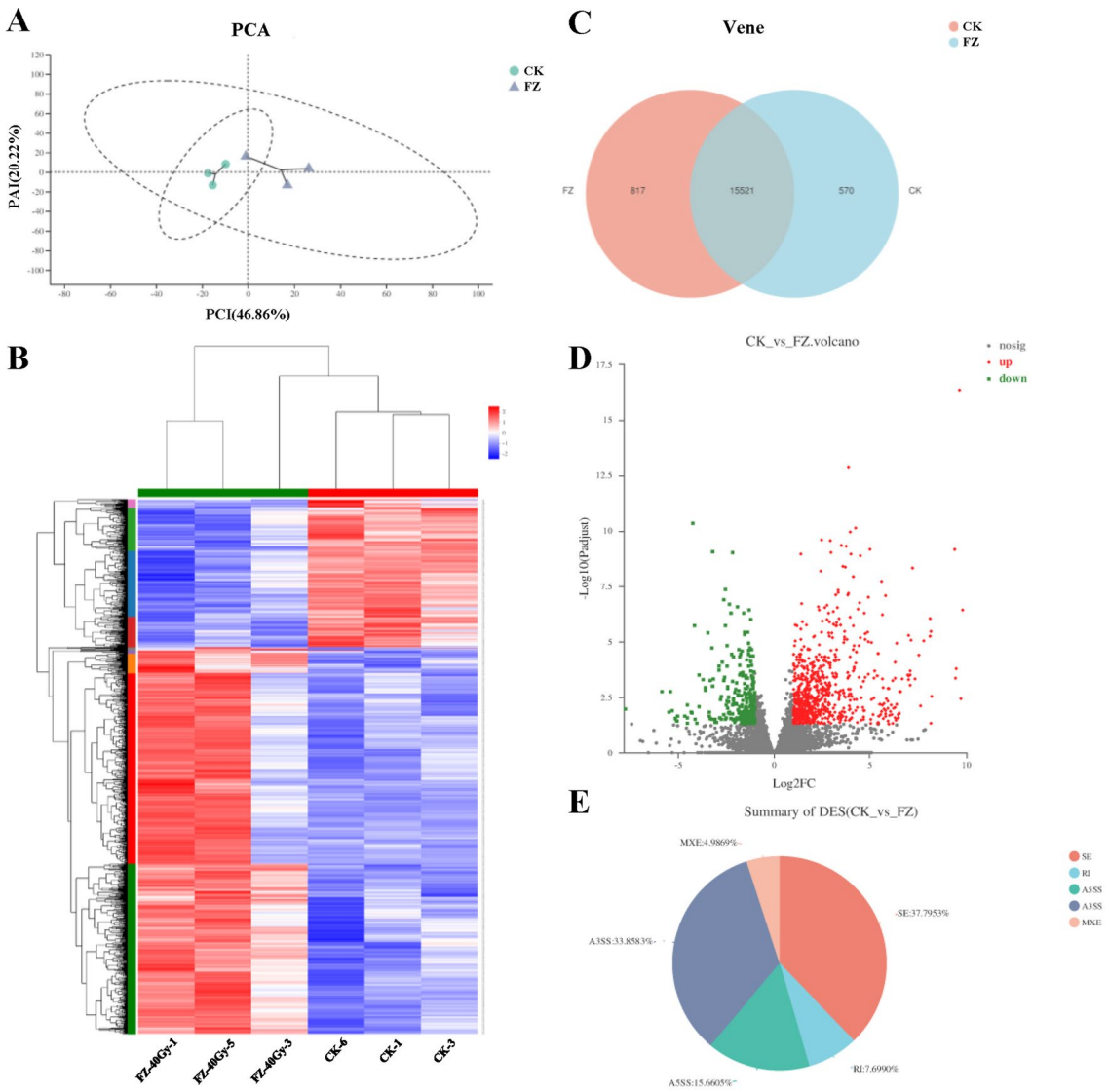

Fig. 2 Statistics of DEGs in RNA-seq. **A** Principal component analysis (PCA) chart. **B** Heat map of DEGs between FZ group and CK group. **C** Venn diagram of the number of DEGs between the FZ group and the CK group. **D** Volcanic map of DEGs in FZ and CK group. **E** Differential gene map with variable shear

40 Gy irradiation treatment, the DEGs related to the regulated synthesis of antioxidant enzymes mediating ROS homeostasis were analyzed (Fig. 5A). Compared with CK samples, peroxidase (LOC110032151, LOC110021580, LOC110021581, and LOC110027479), superoxide dismutase (LOC110031523 and LOC110019501), ascorbate oxidase (LOC110020259, and LOC110036698), and ascorbate transporter (LOC110028342) genes were expressed at higher levels in the irradiated group. This may help to explain the increased ROS-scavenging capacity of the irradiated samples. However, the expression of a CAT gene (LOC110025729) decreased in response to the irradiation (Fig. 5A).

Starch, which is an important storage material in plant organs, is produced from soluble sugars. The transcriptome analysis of the irradiated plants revealed significant irradiation-induced increases in the expression of a starch synthase gene (LOC110034665) and genes related to starch, fructose, trehalose, galactose, and sucrose metabolism (LOC110027413, LOC110021337, LOC110027041, LOC110024845, LOC110027033, LOC110037880, and LOC110031226) (Fig. 5, B). Plant cell walls comprise cellulose and pectin. The transcriptome data indicated the irradiation of the plants significantly increased the expression of pectinase genes (LOC110029424, LOC110039337, LOC110033510, LOC110019941, LOC110017824,

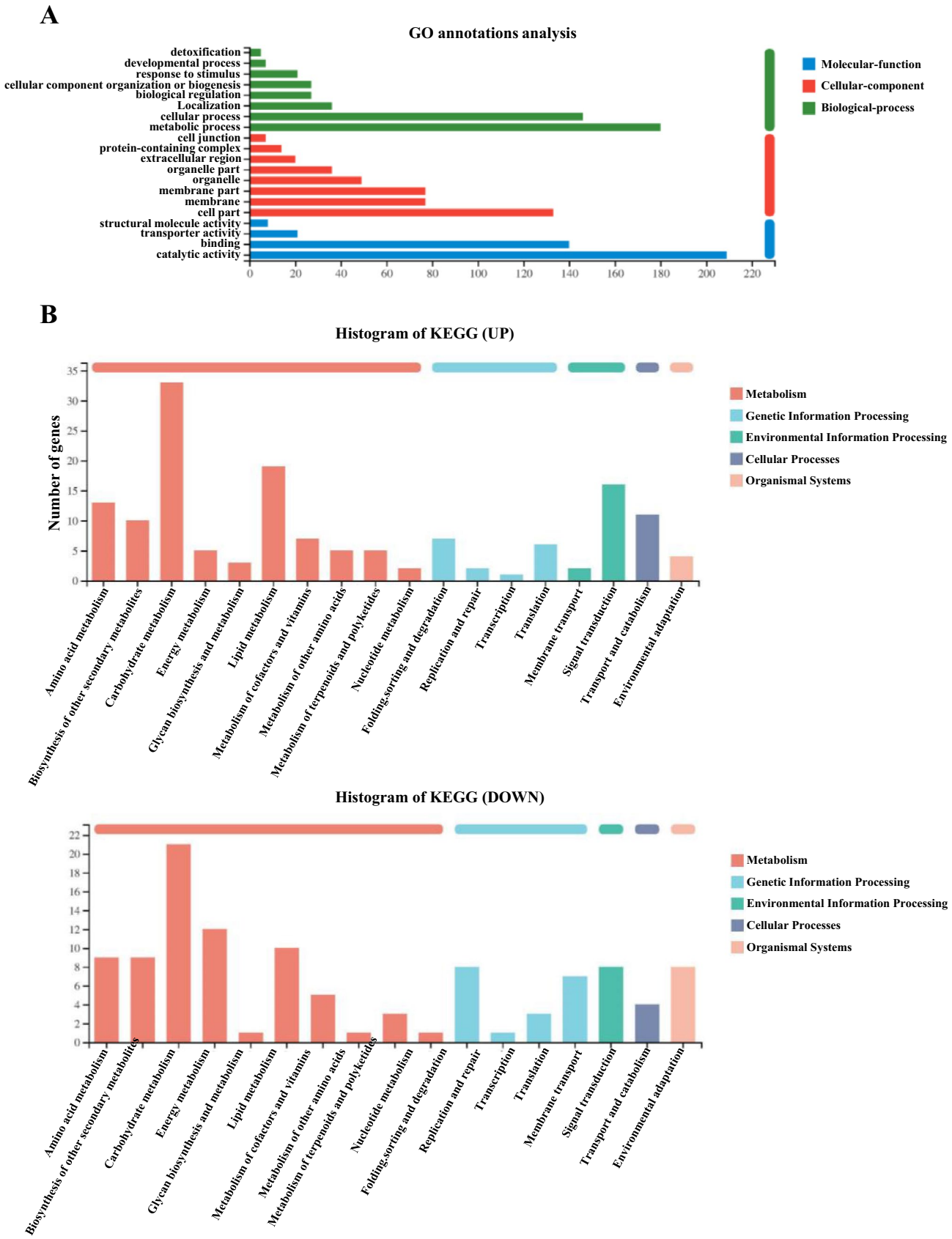

Fig. 3 Annotation analysis of DEGs in RNA-seq. **A** GO classification statistics. **B** KEGG classification statistics

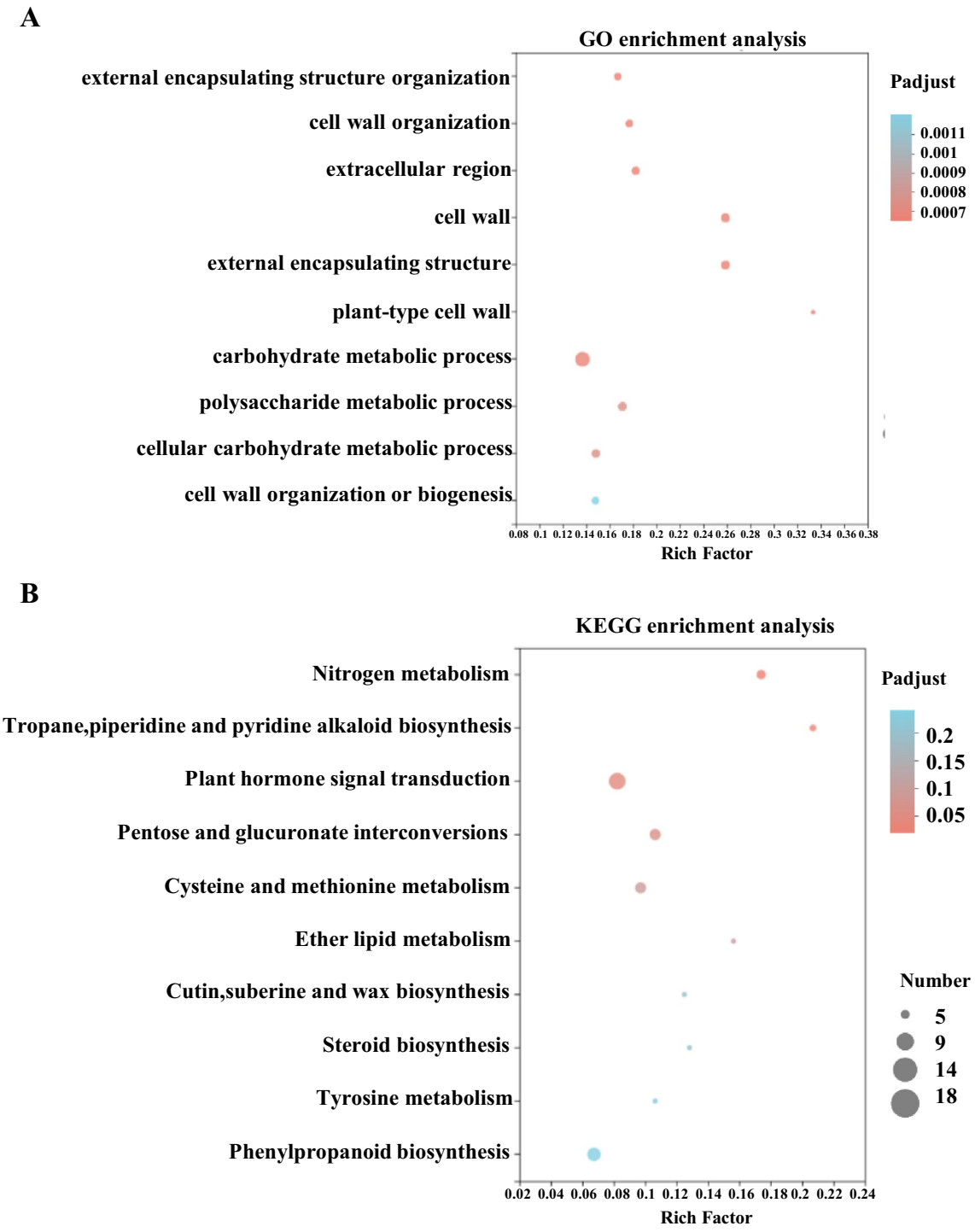

Fig. 4 GO and KEGG enrichment analysis of DEGs in RNA-seq. **A** GO enrichment of DEGs. **B** KEGG enrichment of DEGs

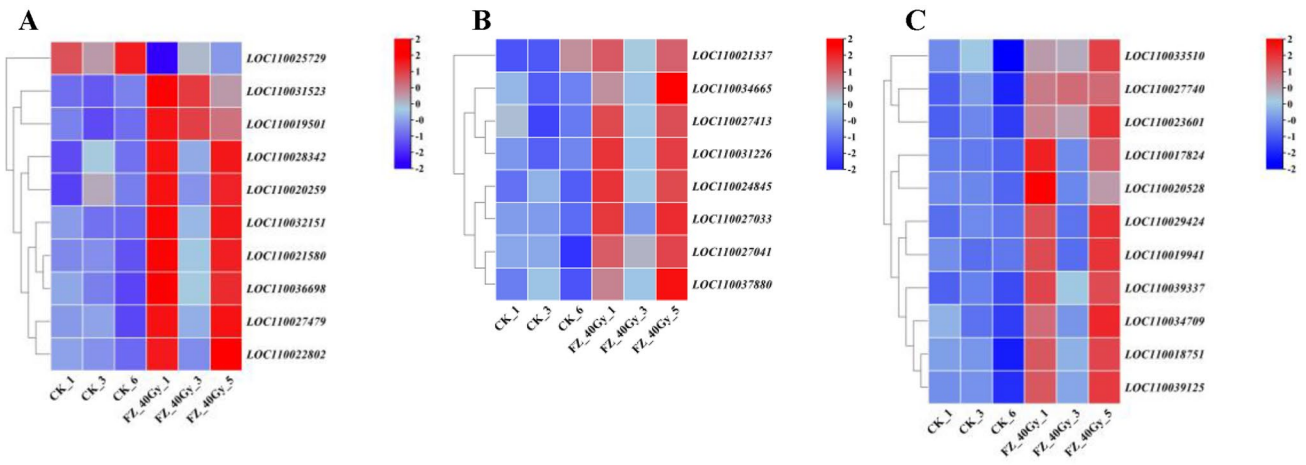

Fig. 5 Analysis of DEGs related to reactive oxygen metabolism pathway and glucose metabolism pathway in RNA-seq. **A** Heat map analysis of DEGs encoding antioxidant enzymes in CK and FZ-40 Gy. **B** Heat map analysis of DEGs encoding glucose metabolism pathway between CK and FZ-40 Gy. **C** Heat map analysis of DEGs encoding pectin and cellulose metabolism between CK and FZ-40 Gy. The related information of genes used for heat map analysis is shown in Supplementary Data Table S2

LOC110018751, and LOC110034709) and cellulase genes (LOC110020528, LOC110039125, LOC110027740, and LOC110023601) (Fig. 5, C).

Transcriptome sequencing analyses identified DEGs related to the rapid plant growth and development after the irradiation

The mechanism mediating the rapid growth of *P. equestris* leaves after the irradiation treatment was elucidated by analyzing the transcriptome data. Rapid leaf development is related to cell proliferation and expansion, the cell division cycle, and the regulation of various growth hormones (Hepworth and Lenhard 2014; Bar and Ori 2014; Vercruysse et al. 2020). Functional genes related to plant hormone signal transduction, plant cell proliferation and expansion, and the cell cycle, were screened. The UniProt website and the available literature were used to clarify gene functions and identify relevant genes (Fig. 6, A). Among the genes in the IAA pathway, the expression levels of auxin response genes (*PeIAA3-1*, *PeIAA3-2*, *PeAUX6B*, *PeAUX22D*, *PeAUX10A*, *PeSAUR64*, and *PeSAUR60*) increased after the irradiation, as did the expression of genes encoding auxin-binding proteins (*PeABP19a-1*, *PeABP19a-2*, and *PeABP19a-3*). The *PeLOG1* gene encodes a cytokinin 5′-phosphoribosyl monophosphate hydrolase, which catalyzes the last step of the bioactive cytokinin synthesis pathway. The expression of this gene increased significantly in the irradiated samples. The expression of *PeHK6*, which encodes a histidine kinase, also increased in the irradiated group. The expression levels of GA regulatory protein-encoding genes (*PeGASA12*, *PeGASA6*, and *PeGASA5*) increased after the irradiation. In the ABA signaling pathway, the expression levels of *PeCYP707A3* (involved in ABA degradation) and *PePYL4* (ABA receptor) increased following the irradiation, which was in contrast to the decreased expression levels of *PePP2C* (activated by ABA) and *PeSAPK10* (involved in ABA signaling). Among the jasmonic acid (JA) signaling pathway genes, the irradiation reduces the expression of *PeJAR1*, which mediates the synthesis of JA, and increases the expression of *PeTRFY10a*, which encodes an inhibitor of jasmonic acid reactions. The expression levels of cyclin genes (*PeCYCA3-1*, *PeCYCD2-2*, *PeCYCD4-1*, and *PeCYCP3-1*) also increased after the irradiation. The expression of *PeNGA* (associated with inhibited cell proliferation) decreased significantly in the irradiated plants, whereas the expression of *PeEXPA10* (related to cell expansion) increased. Ten of these genes (*PeCYCA3-1*, *PeCYCD2-2*, *PeEXPA10*, *PeGAST1*, *PeGASA12*, *PeSAUR50*, *PePP2C*, *PeHK6*, *PeLOG1*, and *PeNGA*) were analyzed by qPCR; the resulting data were consistent with the transcriptome data (Fig. 6, B).

Silencing of *PeEXPA10* resulted in delayed leaf growth

The results of the RNA-seq and qPCR analyses suggested that irradiation significantly promoted the degradation of pectin and cellulose (i.e., cell wall components). We speculated that *PeEXPA10*, which is related to cell wall ductility, may be one of the genes contributing to the rapid growth of leaves. The 40 Gy irradiation increased the *PeEXPA10* expression level. Leaf development was divided into five stages, namely S0, S1, S2, S3, and S4. The *PeEXPA10* gene was highly expressed in the leaves at the S0 stage,

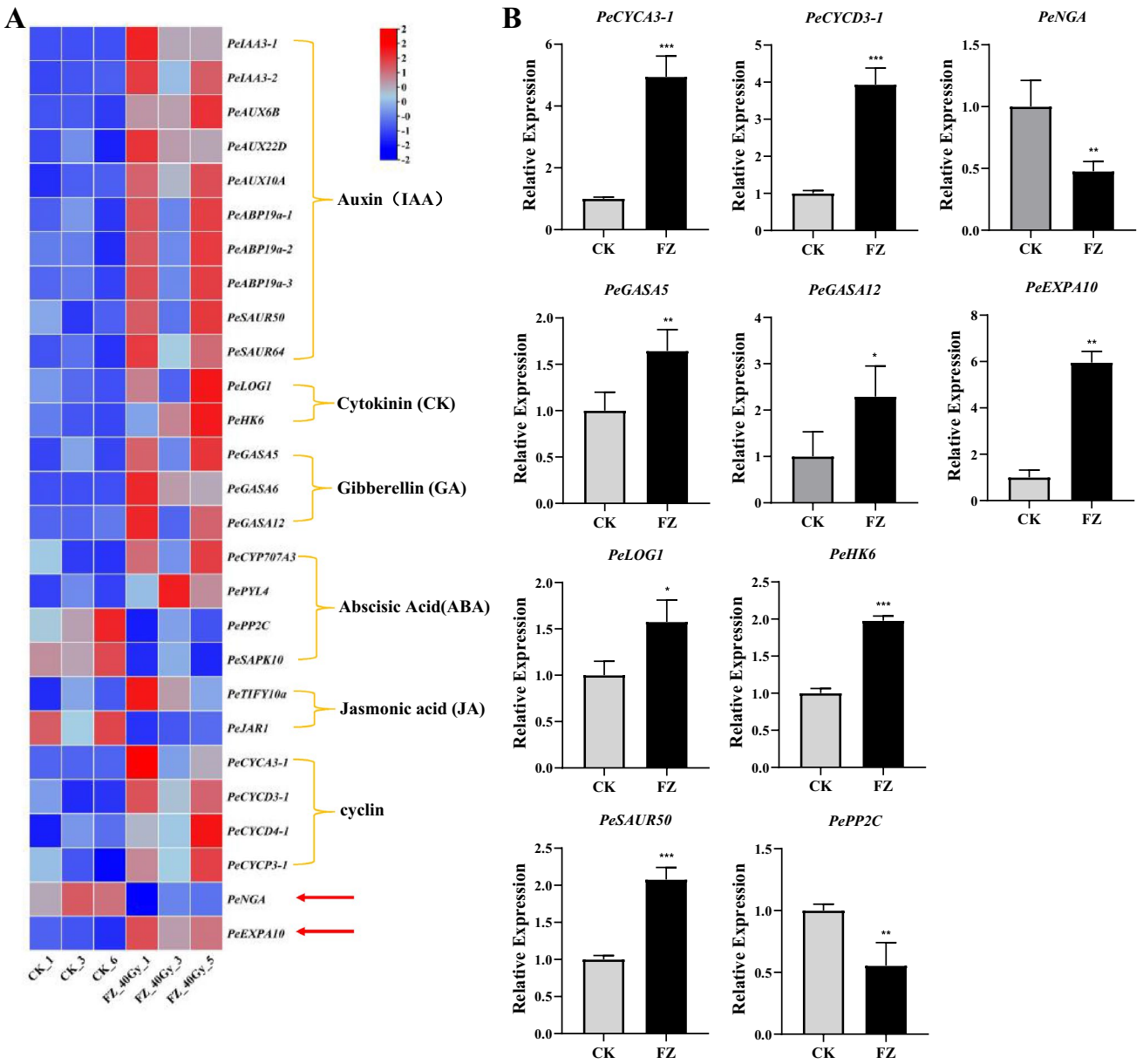

Fig. 6 Screening and expression verification of genes related to leaf development inRNA-seq. **A** Heat map analysis of DEGs in leaf development between CK and FZ-40 Gy (Supplementary Data Table S3). **B** qPCR analysis of DEGs. An asterisk (*) indicates significant differences among treatments (*$p<0.05$; **$p<0.01$. ***$p<0.001$. ****$p<0.0001$). All data were represented as means ± standard deviations (triplicate). Error bars indicate the standard error of the mean

but its expression level decreased as the leaves developed (S0–S4) (Fig. 7A). Virus-induced gene silencing (VIGS) was used to verify the effects of *PeEXPA10* on leaf growth. Specifically, *PeEXPA10* was silenced and the growth of new leaves was observed every 7 days (Fig. 7B). Compared with the CK leaves, the growth rate of the pCymMv-PeEXPA10 leaves decreased significantly in the third week (Fig. 7C). In addition, there were significantly more epidermal cells in the pCymMv-PeEXPA10 plants than in the CK plants (Fig. 7D, E). The qPCR analysis confirmed the *PeEXPA10* expression levels were significantly lower in the pCymMv-PeEXPA10 plants than in the CK plants (Fig. 7F). The qPCR data also indicated that the expression levels of *PeAN*, *PeAPL*, *PeTOR*, and *PeROT3*, which are related to cell expansion, were significantly down-regulated in the pCymMv-PeEXPA10 plants (Fig. 7G).

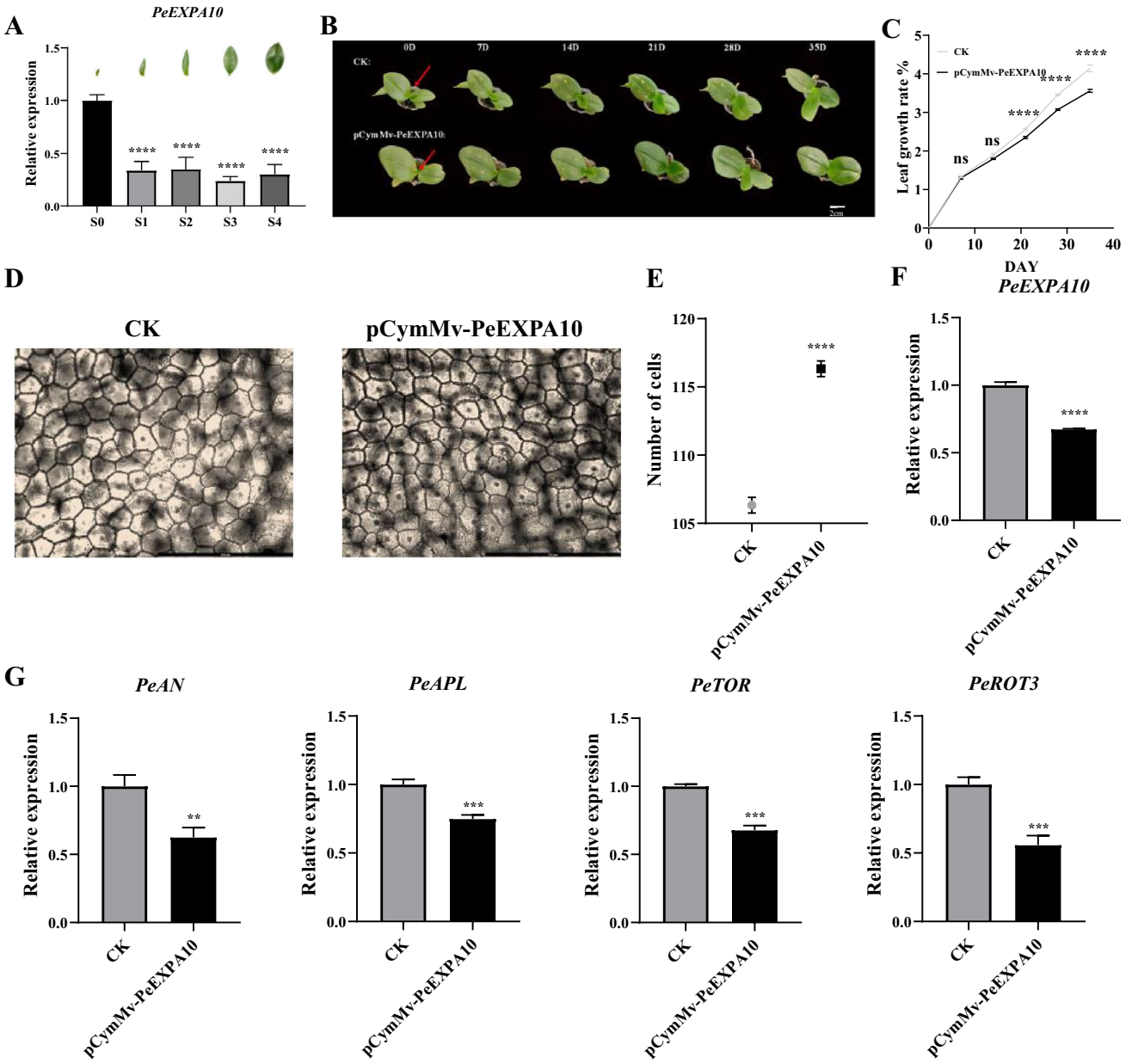

Fig. 7 Functional verification of *PeEXPA10* in Phalaenopsis leaf growth. **A** Relative expression of *PeEXPA10* in leaves at different stages (S0–S4). **B** After infection, the growth status of infected plants was compared with that of no-load control plants (leaves indicated by arrows were the target, and the ratio was 1:1 cm). **C** The growth rate of leaves from day 0 to day 35 after infection. **D** Epidermal cells of leaves of silenced lines and control plants under the microscope (40X microscope). (**E**) The number of epidermal cells was counted. **F** qPCR verification was performed in silenced lines. **G** qPCR analysis of genes in leaves of silenced lines and control plants. An as-terisk (*) indicates significant differences among treatments (*$p<0.05$; **$p<0.01$. ***$p<0.001$. ****$p<0.0001$). All data were represented as means ± standard deviations (triplicate). Error bars indicate the standard error of the mean

Silencing of *PeNGA* accelerated leaf growth

According to the RNA-seq and qPCR analyses, *PeNGA* expression decreased significantly after the irradiation. We hypothesized that *PeNGA* and *PeEXPA10* may have the opposite effects on leaf growth. The expression of *PeNGA* in *P. equestris* leaves at different developmental stages (S0–S4) was analyzed by qPCR (Fig. 8A). The gene was expressed at very low levels at the S0 stage, but its expression level increased from S0 to S4. The involvement of *PeNGA* in leaf growth and development was examined via VIGS. The pCymMv-PeNGA vector was constructed

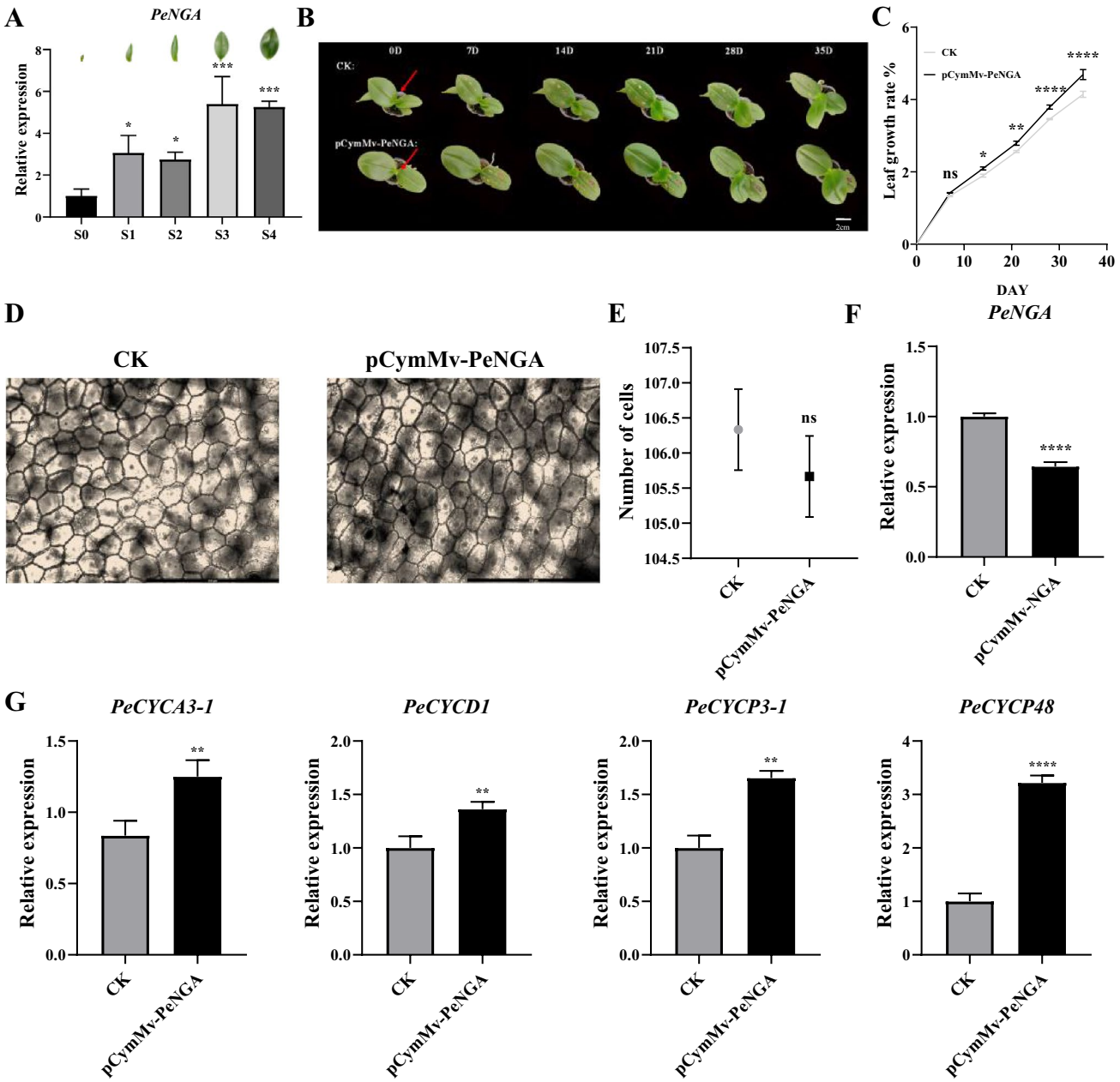

Fig. 8 Functional verification of *PeNGA* in *Phalaenopsis* leaf growth. **A** Relative expression of *PeNGA* in leaves at different periods (S0–S4). **B** After infection, the growth status of infected plants was compared with that of no-load control plants (leaves indicated by arrows were the target, and the ratio was 1:1 cm). **C** The growth rate of leaves from day 0 to day 35 after infection. **D** Epidermal cells of leaves of silenced lines and control plants under the microscope (20X microscope). **E** The number of epidermal cells was counted. **F** qPCR verification was performed in silenced lines. **G** qPCR analysis of genes in leaves of silenced lines and control plants. An asterisk (*) indicates significant differences among treatments (*$p<0.05$; **$p<0.01$. ***$p<0.001$. ****$p<0.0001$). All data were represented as means ± standard deviations (triplicate). Error bars indicate the standard error of the mean

to silence *PeNGA* expression in *P. equestris*, after which the growth of new leaves was analyzed every 7 days (Fig. 8B). The leaf growth rate was significantly higher for the pCymMv-PeNGA plants than for the CK plants in the second week (Fig. 8C). There was no significant difference in the number of epidermal cells between the pCymMv-PeNGA and CK plants (Fig. 8D, E). Accordingly, leaf growth was due to cell proliferation rather than cell expansion. The significant decrease in *PeNGA* expression in the pCymMv-PeNGA plants was verified by the

qPCR analysis (Fig. 8F). Furthermore, the cyclin gene (*PeCYCA3-1*, *PeCYCD1*, *PeCYCP3-1*, and *PeCYCP48*) expression levels were significantly up-regulated in the pCymMv-PeNGA plants (Fig. 8G).

Discussion

Radiation breeding, a method of physical mutagenesis breeding, can generate new germplasm of rare mutants that are challenging to obtain through other techniques (Yamaguchi, 2018). In this study, *P. equestris* was exposed to 40 Gy of ^{60}Co-γ rays, resulting in rapid leaf growth (Fig. 1A, B). The malondialdehyde content and the activities of SOD, POD, CAT, and GPX in the irradiated materials showed significant increases. Carbohydrates, essential energy sources, play a crucial role in plant growth and development (Zhang et al. 2019). RNA-seq analysis of DEGs in irradiated mutagenized plants and the CK revealed a significant increase in genes associated with starch synthesis in leaves. The expressions of genes related to starch, sucrose, galactose, and fructose metabolism were also significantly elevated, suggesting an acceleration in plant growth and metabolic rate (Fig. 5B).

Plant growth and development are intricately linked to the regulation of hormone network factors. Reduction in abscisic acid concentration in plants can decelerate leaf senescence (Xue et al. 2010). Transcriptome analysis of irradiated plants revealed significant differential expression of ABA signaling pathway genes (*PeCYP707A3*, *PePYL4*, *PePP2C*, and *PeSAPK10*) (Fig. 6A), all of which have been reported to play a role in leaf development in previous studies (Spartz et al. 2014; Santiago et al. 2009; Han et al. 2017). In the CK, significant genes involved in leaf development (*PeHK6*, *PeLOG1*) were also identified (Fig. 6A) (Kuroha et al. 2009; Choi et al. 2012). Auxin influences cell division, extension formation, and differentiation, serving as a signal for cell proliferation to determine the final size and shape of organs (Leyser 2001). Transcriptome analysis of IAA signaling pathway genes (*PeIAA3-1*, *PeIAA3-2*, *PeAUX6B*, *PeAUX22D*, *PeAUX10A*, *PeSAUR64*, and *PeSAUR60*) (Fig. 6A) revealed their key role in leaf development, as reported in previous studies (Hou et al. 2013; Kant et al. 2009; Chae et al. 2012). Additionally, significant up-regulation of auxin-binding proteins (*PeABP19a-1*, *PeABP19a-2*, and *PeABP19a-3*) was observed after irradiation (Fig. 6A). Gibberellic acid (GA), a plant hormone belonging to diterpenes, plays a crucial role in the entire life cycle of plants, promoting cell elongation and differentiation (Davière et al. 2008). The transcriptome revealed upregulation of GA signaling pathway genes (*PeGASA12*, *PeGASA6*, and *PeGASA5*) (Fig. 6A), with GASA genes potentially playing a significant role in leaf development, as indicated in previous studies (Zhang and Wang 2017; Zhong et al. 2015; Sun et al. 2013). Jasmonic acid has a clear inhibitory effect on plant seedling growth, particularly in the inhibition of leaf growth (Dathe et al. 1981). Additionally, JA pathway genes (*PeJAR1*, *TRFY10a*) were significantly expressed (Fig. 6A), and they also play a crucial role in leaf development (Wasternack and Jasmonates 2013). It can be inferred that IAA, GA, and CK may promote rapid leaf growth, while ABA and JA play inhibitory roles.

Cellulose and pectin are the primary components of the plant cell wall. Increased levels of cellulase and pectinase enhance plant cell plasticity, resulting in cell wall loosening, which in turn promotes cell expansion and increases the leaf area of the plant (Anderson 2019). Transcriptome data analysis revealed a significant increase in the expression levels of genes related to pectinase and cellulase (Fig. 4 C). *PeEXPA10* plays a crucial role in regulating cell wall expansion. *EXP10* is a non-enzymatic, cell wall-active protein that can relax plant cell walls (Kende et al. 2004). Previous studies have demonstrated that plants ectopically expressing *EXP10* exhibit larger leaves and longer petioles with more giant cells, while downregulation of *EXP10* has the opposite effect (Cosgrove 2015). Following irradiation, the expression of *PeEXPA10* increased, potentially in relation to the elevated levels of pectinase and cellulase, leading to cell wall relaxation and leaf enlargement. This study observed a significantly lower growth rate in *PeEXPA10* gene-silenced plants compared to the CK (Fig. 7C), with the epidermal cells becoming notably smaller (Fig. 7D). These findings suggest that the absence of the *PeEXPA10* gene diminished cell expansion capability, resulting in smaller leaves. It has been reported that the reduction of *PP2C* leads to the activation of cell wall-associated EXP through extracellular acidification induced by auxin, an ATPase that imports H + ions and can promote cell wall loosening. However, further investigation is required to elucidate these mechanisms (Spartz et al. 2014). After irradiation, the expression of the negatively regulated transcription factor *PeNGA* decreased. The growth rate of *PeNGA* gene-silenced plants was significantly higher than that of the CK (Fig. 8C). There was no significant change in cell size (Fig. 8D). In Arabidopsis thaliana, increased petals in nga1-1 mutants were also attributed to increased cell number, indicating that *AtNGA1* may serve as a negative regulator of cell proliferation in lateral organs. In this study, qPCR analysis revealed a significant increase in the expression of cyclin in the silenced lines (Fig. 8G). Therefore, the deletion of the *PeNGA* gene may have alleviated the restriction on cell proliferation, resulting in an accelerated cell proliferation rate. The transcriptome analysis showed that the expression levels of cyclin genes *PeCYCA3-1*, *PeCYCD2-2*, *PeCYCD4-1*, and *PeCYCP3-1* increased (Fig. 8G). Cyclin (CYC) and Cyclin-dependent kinase (CDK) are the central regulators of the plant cell cycle (Jackson 2008). These genes primarily participate in

the G1 phase and the transition from G1 to S phase, playing a crucial role in cell cycle regulation (Vandepoele et al. 2002).

Based on previous research progress and literature reports, combined with our results, we have determined that *PeEXPA10* may function downstream of the abscisic acid pathway and affect the structure of the cell wall. It may also play a role in hormonal pathways, glucose metabolism and reactive oxygen metabolism pathways. Moreover, cell division and proliferation occur continuously and cross various developmental pathways. We have screened the *PeNGA* gene and verified its association with cell division in plants. Although we have only listed the TCP-NGA and cytokinesis pathways in the model, there is still a relationship with the hormone pathway, reactive oxygen metabolism pathway, and sugar metabolism pathway. The individual developmental pathways of plants are complex and interconnected. In conclusion, the developmental process of plants is a complex and extensive network, and we have only partially predicted and verified gene functions. Further studies are needed to explore this topic in greater depth.

This study focused on the rapid growth phenotype and the physiological and metabolic changes in leaves induced by ^{60}Co-γ-40 Gy irradiation. RNA-seq technology was employed to identify key regulatory genes associated with plant hormone signal transduction, glucose metabolism, reactive oxygen species metabolism, and leaf development in response to irradiation stress. Based on the findings, a pathway model of irradiated leaf development was simulated (Fig. 9). Further research is needed to understand how these identified genes regulate the cell cycle for proliferation and expansion. The essential role of *PeNGA* and *PeEXPA10* in rapid leaf development was demonstrated using VIGS technology. However, further investigation is needed to understand the intricate molecular regulatory mechanisms underlying ^{60}Co-γ-40 Gy irradiated mutagenesis, particularly in relation to the interaction between genes and transcription factors, as well as the regulatory dynamics between plant hormones during leaf development. Additionally, it would be intriguing to explore the feasibility of concurrent cell wall expansion and cell proliferation, and to elucidate the coordination and antagonism among key genes. Irradiation offers a promising avenue for plant breeding, yet the underlying mechanisms of this phenomenon warrant continued exploration in the future.

Conclusions

This study revealed the effects of ^{60}Co-γ-40 Gy irradiation on leaf development and physiological metabolism of *Phalaenopsis*. In addition, we used RNA-seq to demonstrate that the differential expression of glucose metabolism genes,

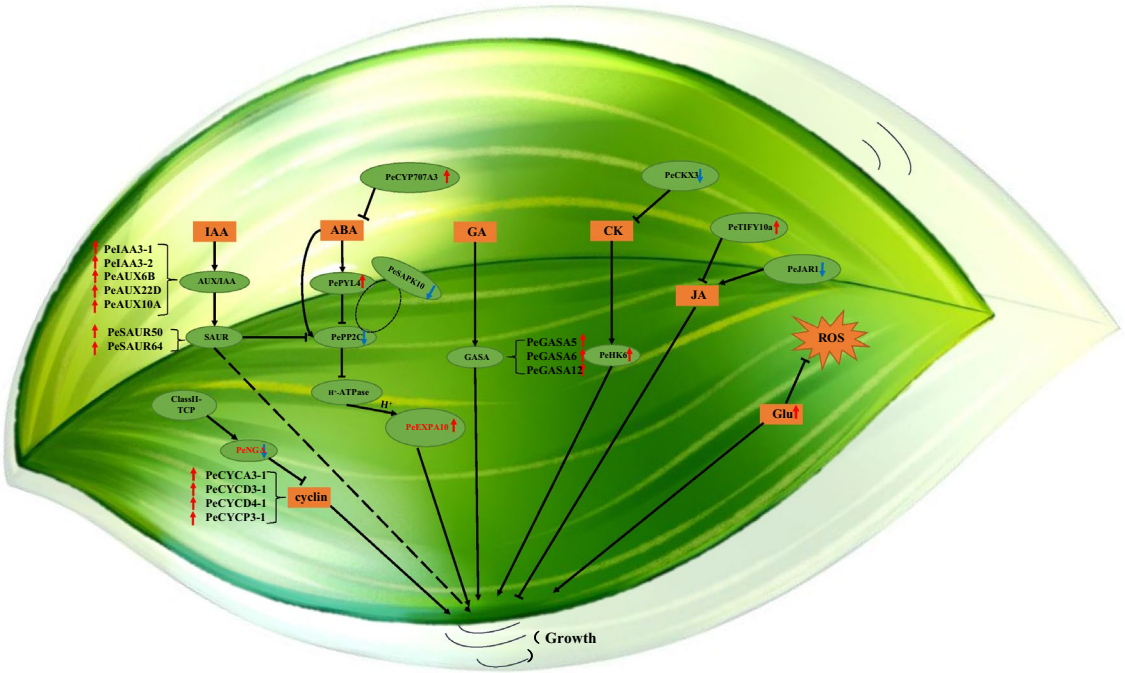

Fig. 9 Leaf development pathway model of P equestris. Red arrows indicate genes with increased expression after irradiation, while blue arrows indicate genes with decreased expression after irradiation

ROS metabolism genes, and leaf development-related genes in irradiated leaves led to these changes. The VIGS technique also confirmed that *PeNGA* and *PeEXPA10* play an essential role in the growth and development of *phalaenopsis* leaves. Therefore, the interaction and regulation between genes and transcription factors after ^{60}Co-γ-40 Gy radiation mutagenesis and the molecular regulatory mechanism of leaf growth and development need to be further studied.

Supplementary Information The online version contains supplementary material available at https://doi.org/10.1007/s00438-024-02102-z.

Author contributions FM conceived the project and designed the study; YM and WL performed the experiments, analyze data and wrote the article; DP and GH provided technical assistance to YM and YG; WL, and ZS test the physiological indexes of the materials after irradiation; YM, YXG, FM and DP revised the article. All of the authors discussed the results and commented on the manuscript.

Funding This work was supported by the National Key Research and Development Program (grant 2018YFD1000400, Ministry of Science and Technology of the People's Republic of China); Ning xia Hui Autonomous Region key research and development program (2022BBF02041); Shanghai Engineering Research Center of Plant Germplasm Resources (17DZ2252700).

Data availability Data will be made available on request.

Declarations

Conflict of interest The authors declare that they have no competing interests. The authors declare that they have no known competing financial interests or personal relationships that could have appeared to influence the work reported in this paper.

References

Aguilar-Martínez JA, Sinha N (2013) Analysis of the role of *Arabidopsis* class I TCP genes AtTCP7, AtTCP8, AtTCP22, and AtTCP23 in leaf development. Front Plant Sci 4:406

Alarkon K, Bozova L, Stoeva N (1987) Index of earliness in tomato plants produced by irradiation of seeds and transplants with gamma rates. Rastenievyd Nauk 24(2):40–43

Alvarez JP, Goldshmidt A, Efroni I et al (2009) The NGATHA distal organ development genes are essential for style specification in *Arabidopsis*. Plant Cell 21(5):1373–1393

Anders S, Huber W (2012) Differential expression of RNA-Seq data at the gene level–the DESeq package. Heidelb Ger: Eur Mol Biol Lab (EMBL) 10:f1000research

Anderson CT (2016) We be jammin': an update on pectin biosynthesis, trafficking and dynamics. J Exp Bot 67(2):495–502

Anderson CT (2019) Pectic polysaccharides in plants: structure, biosynthesis, functions, and applications. Extracellular sugar-based biopolymers matrices. Springer, Cham, pp 487–514

Ballester P, Navarrete-Gómez M, Carbonero P et al (2015) Leaf expansion in Arabidopsis is controlled by a TCP-NGA regulatory module likely conserved in distantly related species. Physiol Plant 155(1):21–32

Bar M, Ori N (2014) Leaf development and morphogenesis. Development 141(22):4219–4230

Calabrese EJ, Baldwin LA (2000) Radiation hormesis: the demise of a legitimate hypothesis. Hum Exp Toxicol 19(1):76–84

Chae K, Isaacs CG, Reeves PH et al (2012) *Arabidopsis* SMALL AUXIN UP RNA63 promotes hypocotyl and stamen filament elongation. Plant J 71(4):684–769

Charbaji T, Nabulsi I (1999) Effect of low doses of gamma irradiation on in vitro growth of grapevine. Plant Cell Tissue Organ Cult 57(2):129–132

Choi J, Lee J, Kim K et al (2012) Functional identification of OsHk6 as a homotypic cytokinin receptor in rice with preferential affinity for iP. Plant Cell Physiol 53(7):1334–1343

Cosgrove DJ (2015) Plant expansins: diversity and interactions with plant cell walls. Curr Opin Plant Biol 25:162–172

Dathe W, Rönsch H, Preiss A et al (1981) Endogenous plant hormones of the broad bean, *Vicia faba* L. (-)-jasmonic acid, a plant growth inhibitor in pericarp. Planta 153(6):530–535

Davière JM, De Lucas M, Prat S (2008) Transcriptional factor interaction: a central step in DELLA function. Curr Opin Genet Dev 18(4):295–303

Demura T, Ye ZH (2010) Regulation of plant biomass production. Curr Opin Plant Biol 13(3):298–303

Fourquin C, Ferrándiz C (2014) The essential role of NGATHA genes in style and stigma specification is widely conserved across eudicots. New Phytol 202(3):1001–1013

Givnish TJ, Spalink D, Ames M et al (2016) Orchid historical biogeography, diversification, Antarctica and the paradox of orchid dispersal. J Biogeogr 43(10):1905–1916

Gonzalez N, Vanhaeren H, Inzé D (2012) Leaf size control: complex coordination of cell division and expansion. Trends Plant Sci 17(6):332–340

Han S, Min MK, Lee SY et al (2017) Modulation of ABA signaling by altering VxGΦL motif of PP2Cs in *Oryza sativa*. Mol Plant 10(9):1190–1205

Hepworth J, Lenhard M (2014) Regulation of plant lateral-organ growth by modulating cell number and size. Curr Opin Plant Biol 17:36–42

Hou K, Wu W, Gan SS (2013) SAUR36, a small auxin up RNA gene, is involved in the promotion of leaf senescence in *Arabidopsis*. Plant Physiol 161(2):1002–1009

Jackson PK (2008) The hunt for cyclin. Cell 134(2):199–202

Kalve S, De Vos D, Beemster GTS (2014) Leaf development: a cellular perspective. Front Plant Sci 5:362

Kant S, Bi YM, Zhu T et al (2009) SAUR39, a small auxin-up RNA gene, acts as a negative regulator of auxin synthesis and transport in rice. Plant Physiol 151(2):691–701

Kende H, Bradford KT, Brummell DA et al (2004) Nomenclature for members of the expansin superfamily of genes and proteins. Plant Mol Biol 55:311–314

Kovacs E, Keresztes A (2002) Effect of gamma and UV-B/C radiation on plant cells. Micron 33(2):199–210

Kuroha T, Tokunaga H, Kojima M et al (2009) Functional analyses of LONELY GUY cytokinin-activating enzymes reveal the importance of the direct activation pathway in *Arabidopsis*. Plant Cell 21(10):3152–3169

Kwon SH, Lee BH, Kim EY et al (2009) Overexpression of a *Brassica rapa* NGATHA gene in *Arabidopsis thaliana* negatively affects cell proliferation during lateral organ and root growth. Plant Cell Physiol 50(12):2162–2173

Leyser O (2001) Auxin signalling: the beginning, the middle and the end. Curr Opin Plant Biol 4(5):382–386

Li H S, Sun Q, Zhao S J, et al (2000) Principles and techniques of plant physiological biochemical experiment. High Educ Beijing, 195–197.

Li C, Dong N, Zhao Y et al (2021) A review for the breeding of orchids: current achievements and prospects. Hortic Plant J 7(5):380–392

Lin CS, Hsu CT, Liao DC et al (2016) Transcriptome-wide analysis of the MADS-box gene family in the orchid *Erycina pusilla*. Plant Biotechnol J 14(1):284–298

Maity JP, Mishra D, Chakraborty A et al (2005) Modulation of some quantitative and qualitative characteristics in rice (*Oryza sativa* L.) and mung (*Phaseolus mungo* L.) by ionizing radiation. Radiat Phys Chem 74(5):391–394

Qi X, Zhu Y, Li S et al (2020) Identification of genes related to mesocarp development in cucumber. Hortic Plant J 6(5):293–300

Saidi A, Hajibarat Z (2021) Phytohormones: Plant switchers in developmental and growth stages in potato. J Genet Eng Biotechnol 19(1):1–17

Santiago J, Rodrigues A, Saez A et al (2009) Modulation of drought resistance by the abscisic acid receptor PYL5 through inhibition of clade A PP2Cs. Plant J 60(4):575–588

Singh B, Datta PS (2010) Gamma irradiation to improve plant vigour, grain development, and yield attributes of wheat. Radiat Phys Chem 79(2):139–143

Somerville C, Bauer S, Brininstool G et al (2004) Toward a systems approach to understanding plant cell walls. Science 306(5705):2206–2211

Spartz AK, Ren H, Park MY et al (2014) SAUR inhibition of PP2C-D phosphatases activates plasma membrane H+-ATPases to promote cell expansion in *Arabidopsis*. Plant Cell 26(5):2129–2142

Sun S, Wang H, Yu H et al (2013) GASA14 regulates leaf expansion and abiotic stress resistance by modulating reactive oxygen species accumulation. J Exp Bot 64(6):1637–1647

Szymanski DB, Cosgrove DJ (2009) Dynamic coordination of cytoskeletal and cell wall systems during plant cell morphogenesis. Curr Biol 19(17):R800–R811

Trigueros M, Navarrete-Gómez M, Sato S et al (2009) The NGATHA genes direct style development in the *Arabidopsis* gynoecium. Plant Cell 21(5):1394–1409

Tsukaya H (2014) Comparative leaf development in angiosperms. Curr Opin Plant Biol 17:103–109

Upton AC (2001) Radiation hormesis: data and interpretations. Crit Rev Toxicol 31(4–5):681–695

Vandepoele K, Raes J, De Veylder L et al (2002) Genome-wide analysis of core cell cycle genes in *Arabidopsis*. Plant Cell 14(4):903–916

Vercruysse J, Baekelandt A, Gonzalez N et al (2020) Molecular networks regulating cell division during *Arabidopsis* leaf growth. J Exp Bot 71(8):2365–2378

Wasternack C, Hause B (2013) Jasmonates: biosynthesis, perception, signal transduction and action in plant stress response, growth and development. An update to the 2007 review in annals of botany. Ann Bot 111(6):1021–1058

Wei X, Liu F, Chen C et al (2014) The Malus domestica sugar transporter gene family: identifications based on genome and expression profiling related to the accumulation of fruit sugars. Front Plant Sci 5:569

Williamson RE, Burn JE, Birch R et al (2001) Morphology ofrsw1, a cellulose-deficient mutant of *Arabidopsis thaliana*. Protoplasma 215(1):116–127

Xue-Xuan X, Hong-Bo S, Yuan-Yuan M et al (2010) Biotechnological implications from abscisic acid (ABA) roles in cold stress and leaf senescence as an important signal for improving plant sustainable survival under abiotic-stressed conditions. Crit Rev Biotechnol 30(3):222–230

Yamaguchi H (2018) Mutation breeding of ornamental plants using ion beams. Breed Sci 68:17086

Yamaguchi T, Yano S, Tsukaya H (2010) Genetic framework for flattened leaf blade formation in unifacial leaves of *Juncus prismatocarpus*. Plant Cell 22(7):2141–2155

Young MD, Wakefield MJ, Smyth GK et al (2010) Gene ontology analysis for RNA-seq: accounting for selection bias. Genome Biol 11(2):1–12

Zhang S, Wang X (2017) One new kind of phytohormonal signaling integrator: up-and-coming GASA family genes. Plant Signal Behav 12(2):e1226453

Zhang JW, Sun JX, Guo WJ et al (2016) Study on the Relationship between leaf growth curve and accumulated temperature of *Phalaenopsis*. Chin Agric Sci Bull 32(1):113–117

Zhang J, Shi X, Liu H, Ma G et al (2018) Study on the differential accumulation of anthocyanin in different-colored phalaenopsis based on transcriptomics. Mol Plant Breed 16(14):4530–4542

Zhang LZ, Zhang X, Zuo XY et al (2019) Effects of exogenous glucose treatment on soluble sugar and expression of related genes during floral bud differentiation stage in terminal spur buds of'Nagafu 2'apple. Acta Hortic Sin 46(1):11–24

Zhong C, Xu H, Ye S et al (2015) Gibberellic acid-stimulated Arabidopsis6 serves as an integrator of gibberellin, abscisic acid, and glucose signaling during seed germination in *Arabidopsis*. Plant Physiol 169(3):2288–2303